OPEN ACCESS
CellPress

Cell Reports
Article

Impaired p32 Regulation Caused by the Lymphoma-Prone RECQ4 Mutation Drives Mitochondrial Dysfunction

Jiin-Tarng Wang,[1] Xiaohua Xu,[1] Aileen Y. Alontaga,[2] Yuan Chen,[2] and Yilun Liu[1,*]
[1]Department of Radiation Biology, Beckman Research Institute, City of Hope, Duarte, CA 91010-3000, USA
[2]Department of Molecular Medicine, Beckman Research Institute, City of Hope, Duarte, CA 91010-3000, USA
*Correspondence: yiliu@coh.org
http://dx.doi.org/10.1016/j.celrep.2014.03.037

SUMMARY

Mitochondrial DNA (mtDNA) encodes proteins that are important for ATP biogenesis. Therefore, changes in mtDNA copy number will have profound consequences on cell survival and proliferation. RECQ4 DNA helicase participates in both nuclear DNA and mtDNA synthesis. However, the mechanism that balances the distribution of RECQ4 in the nucleus and mitochondria is unknown. Here, we show that RECQ4 forms protein complexes with Protein Phosphatase 2A (PP2A), nucleophosmin (NPM), and mitochondrial p32 in different cellular compartments. Critically, the interaction with p32 negatively controls the transport of both RECQ4 and its chromatin-associated replication factor, MCM10, from the nucleus to mitochondria. Amino acids that are deleted in the most common cancer-associated RECQ4 mutation are required for the interaction with p32. Hence, this RECQ4 mutant, which is no longer regulated by p32 and is enriched in the mitochondria, interacts with the mitochondrial replication helicase PEO1 and induces abnormally high levels of mtDNA synthesis.

INTRODUCTION

Mitochondria (MT) are key cellular organelles that generate ATP for diverse cellular processes that are necessary to support cell growth, and deterioration of MT and mtDNA contributes to the aging process (Lee and Wei, 2012). Furthermore, accumulating evidence also suggests there is an intimate connection between MT dysfunction and cancer development (Carew et al., 2004; D'Souza et al., 2007; Jeon et al., 2007; Lan et al., 2008). Because the mtDNA copy number positively correlates with the rate of cell growth (Jeng et al., 2008), deregulated mtDNA synthesis could be a risk factor that contributes to carcinogenesis or sustains the rapid proliferation of cancer cells once they are established. For this reason, in recent years, MT have gained attention both as a potential diagnostic tool and as a therapeutic target for cancer therapy (Yu, 2011).

In mammals, the members of the conserved RECQ helicase family are important for nuclear DNA replication and damage repair, and have also been suggested to participate in mtDNA maintenance (de Souza-Pinto et al., 2010). Among the five RECQ helicases identified, RECQ4, which is an essential gene in vertebrates (Abe et al., 2011; Ichikawa et al., 2002), has been observed in both the nucleus and MT (Chi et al., 2012; Croteau et al., 2012; Yin et al., 2004). Indeed, multiple regions of RECQ4 are required for its nuclear localization (Burks et al., 2007), and it was suggested that a potential MT-targeting signal is located within the first 20 amino acids (De et al., 2012). Mutations in RECQ4 have been linked to three clinical diseases that feature premature-aging phenotypes and a predisposition to develop osteosarcoma and lymphoma (Liu, 2010). Through its unique N terminus, RECQ4 forms chromatin-specific protein complexes that contain the essential nuclear replication factors MCM10 and the CDC45-MCM2-7-GINS (CMG) helicase (Xu et al., 2009), and initiate DNA replication (Im et al., 2009; Sangrithi et al., 2005; Thangavel et al., 2010). In addition to reducing nuclear DNA replication, RECQ4 deficiency decreases mtDNA copy number and the energy-production capacity of MT (Chi et al., 2012; Croteau et al., 2012). However, the molecular mechanism that balances the distribution of RECQ4 in the nucleus and MT remains to be defined.

In this study, we identified three RECQ4 interacting proteins: PP2A, NPM, and MT p32. We determined that p32 promotes the nuclear localization of RECQ4 by suppressing its transport to MT. Importantly, the most common cancer-associated *RECQ4* mutation, c.1390+2 delT, which deletes Ala420–Ala463 (Siitonen et al., 2009), produces a protein that cannot interact with p32. Individuals homozygous or compound heterozygous for this internal deletion (ID) in the RECQ4 protein develop RAPADILINO syndrome, and 40% of these patients develop cancers that are primarily lymphomas. We found that the RECQ4 ID mutant protein relocalized from the nucleus to MT, where it accumulated. As a consequence, an excess amount of RECQ4 mutant protein was able to interact with the MT replication helicase PEO1 and led to an increase in mtDNA synthesis, and an enhanced use of the glycolysis pathway in preference to oxidative phosphorylation (OXPHOS). Our data provide insights into how the intracellular location of RECQ4 is regulated, as well as RECQ4's potential link to cancer etiology.

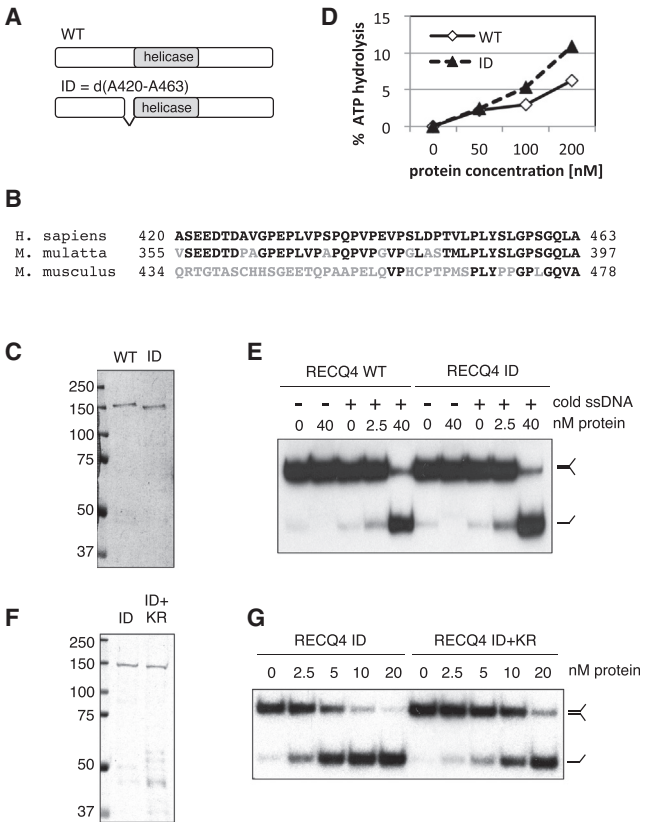

Figure 1. The Lymphoma-Prone RECQ4 ID Mutant Is Catalytically Active

(A) Schematic diagrams of WT RECQ4 and the lymphoma-associated RECQ4 ID mutant, which lacks residues A420–A463. The conserved SFII helicase domain is shown in light gray.

(B) Sequence alignment of the human RECQ4 (A420–A463 aa) with the corresponding regions of the *M. mulatta* and *M. musculus* RECQ4 proteins. Conserved residues are shown in black.

(C) Recombinant WT RECQ4 and ID proteins purified from *E. coli*, separated by SDS-PAGE, and stained with Coomassie blue.

(D) Comparison of the ATPase activities of the WT RECQ4 and ID proteins in the presence of ssDNA.

(E) DNA strand-exchange activities of the WT RECQ4 and ID proteins were measured using ^{32}P-end-labeled splayed-arm substrates in the presence or absence of unlabeled oligos containing the identical sequence to the ^{32}P-end-labeled strand of the splayed arm substrates. The X01 strand of the splay-arm substrate was labeled with ^{32}P.

(F) Recombinant RECQ4 ID and ID-K508R (KR) double mutants purified from *E. coli*, separated by SDS-PAGE, and stained with Coomassie blue.

(G) DNA strand-exchange activities of the RECQ4 ID and ID-K508R (KR) proteins were measured as described in (E).

RESULTS

The Lymphoma-Prone RECQ4 ID Mutant Protein Is Catalytically Active

Ala420–Ala463 residues, which are unique to primates and are missing in the lymphoma-prone RECQ4 ID mutant, are located between the essential N terminus and the conserved Superfamily Helicase Domain II (SFII; Figures 1A and 1B). Structure predictions made using the GOR4 Secondary Structure Prediction Tool and GlobPlot suggest that these residues are disordered and unlikely to affect the folding of the adjacent domains. Indeed, we found that purified recombinant RECQ4 ID protein has ATPase activity similar to that of the wild-type (WT) RECQ4 protein (Figures 1C and 1D). RECQ4 also exhibits strong single-stranded DNA (ssDNA) annealing activity and can efficiently carry out ATP-dependent DNA strand-exchange reactions, such that the ^{32}P-labeled strand of a splayed arm substrate is dissociated as a ssDNA product and replaced by an unlabeled ssDNA containing the same sequence (Figure 1E; Xu and Liu, 2009). Previously, we showed that RECQ4 possesses dual DNA strand-exchange activities: one controlled by the SFII domain and one located within the N-terminal domain (Xu and Liu, 2009). We found that suppressing the SFII domain by introducing the K508R mutation weakened, but did not abolish, the DNA strand-exchange activity (Figures 1F and 1G), indicating that the SFII and N-terminal domains of the RECQ4 ID mutant are both catalytically active.

The Lymphoma-Prone RECQ4 ID Mutant Protein Supports DNA Replication

We next determined the effect of the RECQ4 ID mutant on cell growth and nuclear DNA replication. First, we generated 293T, U2OS, and HT1080 cell lines that stably expressed a RECQ4 short hairpin RNA (shRNA), which, as expected, reduced the proliferation rate of the cells (Figures 2A, 2B, S1A, and S1B). The stable RECQ4 shRNA-knockdown cells were then transfected with shRNA-resistant plasmids that expressed either FLAG-tagged RECQ4 WT or the ID mutant protein at comparable levels (Figures 2C and S1C). The FLAG-tagged RECQ4 proteins were expressed at approximately 2- to 4-fold higher levels compared with the endogenous RECQ4 protein (Figures S2A and S2B). Interestingly, the stable expression of RECQ4 ID, but not the WT protein, was toxic to HT1080 cells. Nevertheless, we found that expressing the ID mutant, but not the vector, facilitated the growth rate of the RECQ4 shRNA knockdown 293T and U2OS cells as efficiently as the WT protein (Figures 2D and S1C). Furthermore, cell-cycle analysis confirmed that the RECQ4 ID cells progressed through S phase at a rate similar to that observed for the cells expressing the WT protein (Figure S3).

Human RECQ4 localizes to both the cytoplasm and the nucleus (Burks et al., 2007; Yin et al., 2004; Figure S2C). Consistent with this, we found that the exogenously expressed FLAG-RECQ4 WT also localized to the cytoplasm and nucleus in various human cell lines (Figure S2D). Previously, it was suggested that the Ala420–Ala463 residues may contain a potential nuclear retention signal (Burks et al., 2007). Indeed, we saw a decreased amount of RECQ4 ID on human chromatin (CB) and a proportional increase of the protein in the cytoplasm (CE; Figure 2E, top two panels). Immunofluorescent microscopy also showed that the nuclear localization of RECQ4 ID mutant was reduced (Figure S4). However, despite the reduction, the mutant was still able to form a complex with the MCM proteins on DNA (Figure 2F). Furthermore, a higher percentage of the RECQ4 ID protein bound to chromatin was in complexes with nuclear replication factors compared with the WT protein (Figure 2F). We suggest that this increase in percentage could compensate for the decreased amount of RECQ4 ID that is chromatin bound. Altogether, our results indicate that the lymphoma-prone

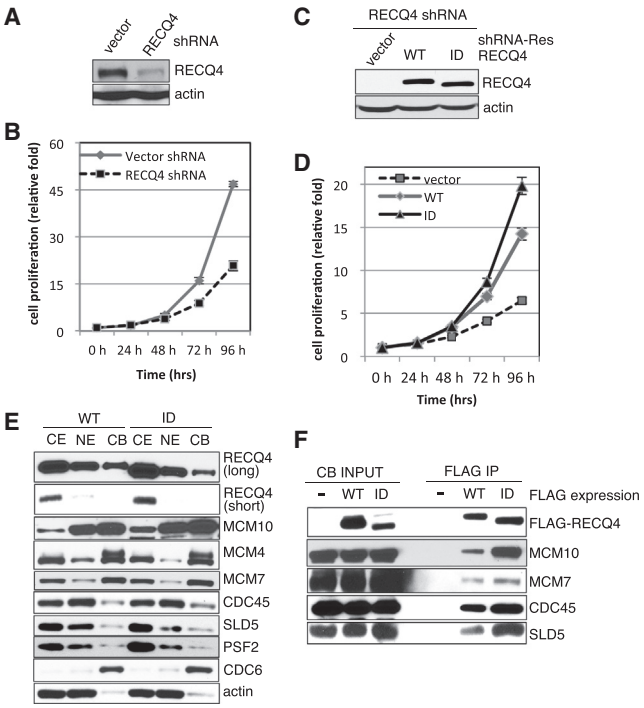

Figure 2. The Lymphoma-Prone RECQ4 ID Mutant Forms CB RECQ4-MCM Complexes and Supports Cell Growth

(A) Protein levels of RECQ4 were analyzed using rabbit RECQ4 antibody on western blots of WCEs prepared from HEK293T cells stably expressing a control vector or RECQ4 shRNA. Actin was used as the loading control.

(B) The effect of RECQ4 knockdown by shRNA on cell growth was measured in crystal violet cell proliferation assays. Results are means ± SDs from three separate wells. Data are representative of three independent experiments.

(C) Protein levels of the WT RECQ4 and ID mutant were analyzed using rabbit RECQ4 antibody on western blots of WCE prepared from RECQ4 shRNA knockdown cells that stably expressed vector alone or shRNA-resistant FLAG-RECQ4 WT or ID mutant protein.

(D) Cell proliferation rates were compared among RECQ4 shRNA knockdown cells complemented with empty vector, an shRNA-resistant WT FLAG-RECQ4 expression construct, or a plasmid expressing the FLAG-RECQ4 ID mutant protein from (C). Results are means ± SDs from three separate wells. Data are representative of three independent experiments.

(E) Protein levels of RECQ4, MCM10, MCM2-7 (represented by MCM4 and MCM7), CDC45, and GINS (represented by SLD5 and PSF2) were analyzed on western blots of CE, NE, and soluble CB fractions that were prepared from WT RECQ4 or ID cells.

(F) Western blots of the immunopurified FLAG complexes from the soluble CB fractions (left three lanes) prepared from cells expressing vector, FLAG-RECQ4 WT, or FLAG-RECQ4 ID. The immunopurified complexes were probed with antibodies to detect RECQ4, MCM10, MCM2-7 (MCM7), CDC45, and GINS (SLD5).

RECQ4 ID mutant protein is capable of forming functional replication helicase complexes that support DNA synthesis and cell growth.

MT Dysfunction in Cells Expressing the RECQ4 ID Mutant Protein

RECQ4 has been implicated in mtDNA maintenance (Chi et al., 2012; Croteau et al., 2012). Indeed, the 293T cells we depleted of RECQ4 contained less mtDNA than control knockdown cells

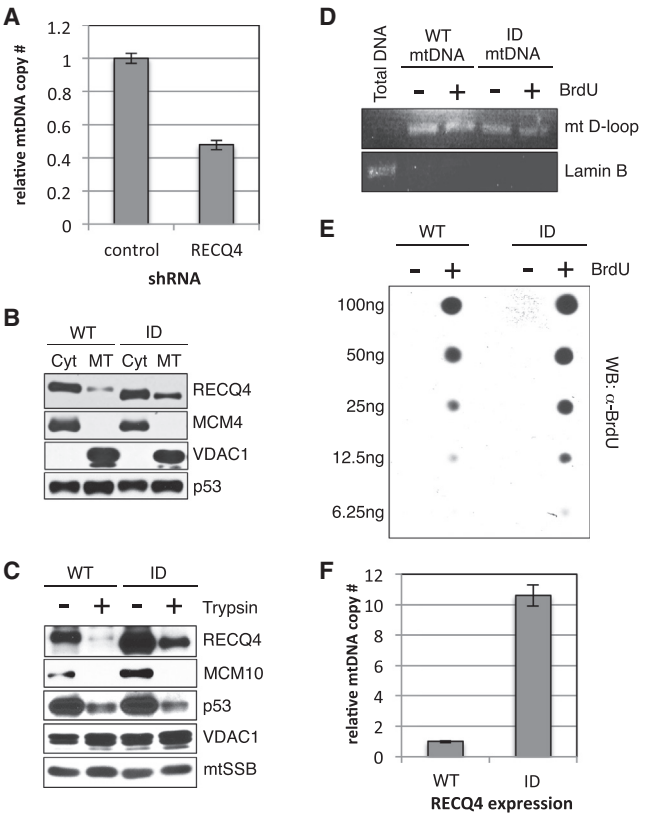

Figure 3. The Lymphoma-Associated RECQ4 ID Mutant Is Enriched in MT and Promotes mtDNA Synthesis

(A) The copy number of mtDNA compared with genomic DNA was quantified in cells stably transfected with control or RECQ4 shRNA. Data are represented as means ± SD from three independent experiments.

(B) MT fractions were isolated from WT RECQ4 or ID cells by centrifuging the CE extracts to pellet the MT. The supernatant that was depleted of MT proteins was collected and designated as the Cyt fraction. Protein levels of RECQ4, MCM2-7 (MCM4), and p53 were analyzed on western blots of the Cyt and MT fractions (5 μg per lane). VDAC1 was used as the loading control of MT.

(C) Protein levels of RECQ4, MCM10, p53, and mtSSB inside the MT were determined by trypsin digest of the intact MT followed by MT lysis and western blotting. Proteins that were resistant to trypsin digest were localized inside the MT; 25 μg of the MT extracts was used in each sample.

(D) PCR analysis to detect nuclear DNA (lower panel, Lamin B) and mtDNA (upper panel, mt D-loop) using DNA template prepared from total genomic DNA (lane 1), purified mtDNA from either RECQ4 WT or ID cells, with or without BrdU labeling (lanes 2–5). For mt D-loop PCR, 3 ng of DNA was used as template, whereas 60 ng of DNA was used for Lamin B PCR.

(E) Dot blot analysis for BrdU in the indicated amounts of mtDNA prepared from either RECQ4 WT or ID cells, with or without BrdU labeling.

(F) mtDNA copy number relative to genomic DNA was quantified in cells expressing either the WT RECQ4 or the ID mutant. Data are represented as means ± SD from three independent experiments.

(Figure 3A). Therefore, we determined whether the increased amount of RECQ4 ID protein in the cytoplasm led to increased MT localization. The CE fraction (Figure 2E) contained both cytosolic (Cyt) and MT proteins. Therefore, we further separated the CE extract into Cyt and MT proteins, and found that the increased amount of RECQ4 ID protein was located primarily in MT (Figures 3B, S5A, and S5B). Trypsin proteolysis of intact

MT confirmed that there was an increased amount of RECQ4 ID protein in the MT matrix (Figure 3C), which is where the mtDNA is located. This result raised the possibility that mtDNA synthesis could be abnormal in RECQ4 ID mutant cells. To test this hypothesis, we isolated mtDNA from WT- and ID-expressing cells that had been pulse labeled with bromodeoxyuridine (BrdU) to monitor DNA synthesis. PCR analysis confirmed that the mtDNA we prepared from these cells contained little contaminating nuclear DNA (Figure 3D). By performing western blotting using a BrdU antibody and comparing equal amounts of purified mtDNA, we found that mtDNA isolated from the ID cells incorporated higher levels of BrdU compared with mtDNA from WT-expressing cells (Figure 3E). This result explained the increased mtDNA copy number we observed in RECQ4 ID cells compared with WT cells (Figures 3F, S5C, and S5D). Interestingly, we found that the difference between the amount of MT WT and ID RECQ4 protein was greatest in HT1080 cells that were transiently transfected with the RECQ4 WT or ID mutant (Figure S5B). In addition, an elevated mtDNA copy number was observed within 2 days of the transient transfection (Figure S5D). These observations may explain why we were unsuccessful in establishing an HT1080 cell line that stably expressed RECQ4 ID protein. There was also an increase in CE MCM10 in the RECQ4 ID cells (Figure 2E), which was due to MCM10 also being enriched in the MT fraction (Figure 3C). Because RECQ4 normally interacts with MCM10 in the nucleus (Xu et al., 2009), the excess RECQ4 ID protein and MCM10 that localized to the MT were most likely transported directly from the nucleus. Nevertheless, trypsin analysis indicated that MCM10 remained at the MT outer membrane and did not enter the matrix (Figure 3C). On the other hand, the localization of p53 to the MT, which is dependent on RECQ4 (De et al., 2012), was unchanged in RECQ4 ID-expressing cells (Figures 3B, 3C, S5A, and S5B).

Overexpression of PEO1 leads to a high mtDNA copy number and mtDNA deletions (Ylikallio et al., 2010), suggesting that rapid mtDNA synthesis could contribute to mtDNA mutagenesis. Because mtDNA encodes components of the OXPHOS complex required for ATP production, increasing the mtDNA copy number could affect the expression or function of the OXPHOS pathway. We used nuclear magnetic resonance (NMR) to analyze the metabolites of total cell extracts, which allowed us to quantitatively measure MT-associated metabolites, such as intermediates of the tricarboxylic citric acid (TCA) cycle that are present at high cellular concentrations. We found that the cellular concentrations of malate, NADH, oxoglutarate, and ATP were decreased in RECQ4 ID cells compared with WT cells (Figures 4A, 4B, and S6). In contrast, lactate and amino acid levels were increased in ID cells (Figures 4A, 4B, and S6), indicating that MT function is reduced in RECQ4 ID cells and there is an elevated rate of glycolysis in the Cyt (Figure 4C). This phenomenon is known as the Warburg effect and is frequently observed in cancer cells (Vander Heiden et al., 2009).

Protein-Protein Interactions with Human RECQ4

Our data indicate that the 44 amino acids missing from the lymphoma-prone RECQ4 ID mutant are required to block its transport from the nucleus to the MT, and we hypothesized that this negative regulation is accomplished via protein-protein interactions. To identify factors that regulate the localization of RECQ4 to MT, we performed a large-scale immunopurification of FLAG-RECQ4 WT protein as previously described (Xu et al., 2009), except that we used the nonchromatin fractions (e.g., a combination of CE and nucleoplasmic [NE] extracts; Figure 5A). We used 293T cells without FLAG protein expression to subtract out nonspecific polypeptides in the immunoprecipitated sample (Figure 5A, left lane), and we identified PP2A, NPM, and MT p32 as the most abundant copurified proteins (Figures 5B and S7). Using antibodies specific to RECQ4, we further confirmed that PP2A, NPM, and p32 copurified with the endogenous RECQ4 proteins in 293T cells (Figure 5C).

PP2A is a serine/threonine phosphatase that is important for regulating cell growth (Janssens and Goris, 2001), and cell fractionation revealed that the majority of PP2A was cytosolic (Figure 5D). NPM is an essential and multifunctional chaperone protein that is known to shuttle among several cellular compartments, including the nucleolus, nucleoplasm, and cytoplasm (Falini et al., 2007). NPM has been implicated in regulating centrosome duplication, chromatin remodeling, ribosome biogenesis, and maintaining genome stability (Lindström, 2011). We found that NPM was predominantly detected in the NE fraction and on the chromatin-bound (CB) fraction (Figure 5D). The p32 protein, also known as gC1qR or HABP1, resides primarily in the MT (Figure 5D), where it is thought to regulate MT innate immune responses, OXPHOS for ATP biogenesis, and protein localization to the MT, such as in the case of the tumor suppressor ARF (Fogal et al., 2010; Itahana and Zhang, 2008; Muta et al., 1997; West et al., 2011). Nonetheless, even though each of these RECQ4-interacting proteins seemed to concentrate in distinct cellular compartments, they appeared to be mobile and could also be present in multiple cellular compartments (Figure 5D).

Next, we determined the cellular compartments in which RECQ4 interacted with these proteins by immunopurifying FLAG-RECQ4 from the Cyt, MT, NE, and CB fractions. We asked which RECQ4-interacting proteins were enriched in RECQ4 complexes purified from specific cellular compartments when compared with RECQ4 complexes purified from whole-cell extracts (WCEs). We found that PP2A, which is located primarily in the Cyt (Figure 5D), was detected mainly in the Cyt RECQ4 complex (Figure 5E). The most stable interaction between p32 and RECQ4 was found in the MT (Figure 5F). NPM, which was found mostly in the nucleus, interacted with RECQ4 primarily in the NE (Figure 5G) but could also associate with CB RECQ4 (Figure 5H). Previously, NPM was not detected in purified RECQ4 CB complexes, which were isolated after a standard 2 hr benzonase digestion of the chromatin pellet (Xu et al., 2009). The CB RECQ4-NPM complex was only detected when the chromatin was digested with benzonase overnight, suggesting that CB RECQ4-NPM complexes are likely to be tightly associated with condensed regions of the chromosomes, such as heterochromatin. Interestingly, even though MCM10 interacted preferentially with RECQ4 on chromatin (Figure 5H), a weak amount of MCM10 was detected in the MT RECQ4 complex (Figure 5F). This is consistent with our observation that suggests MCM10 can be cotransported to the MT with RECQ4.

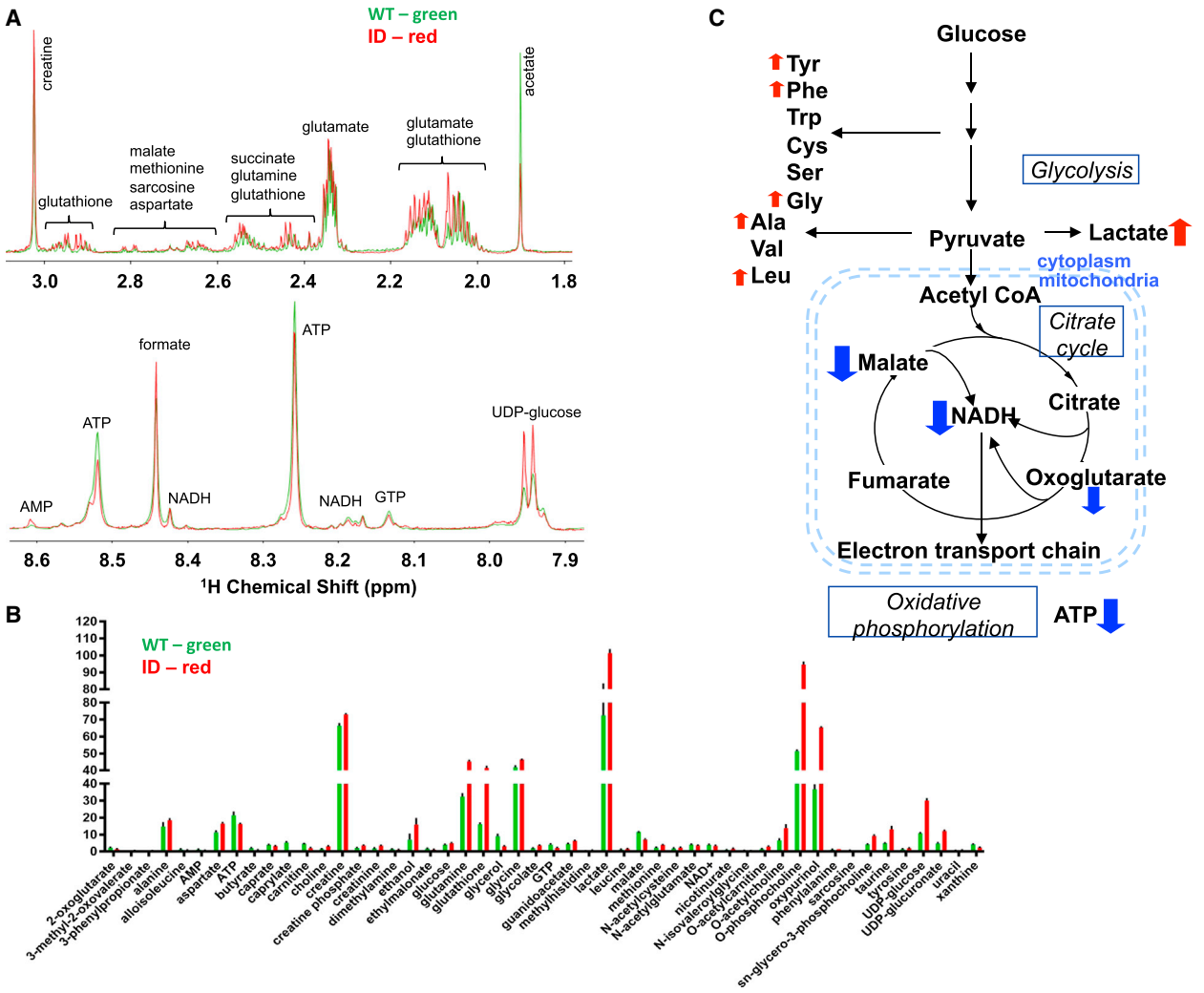

Figure 4. RECQ4 WT and ID Cells Exhibit Different MT Metabolic Profiles

(A) Representative ^{1}H NMR spectra of the hydrophilic metabolites extracted from WT (green) and ID mutant (red) cells with expanded upfield (top) and downfield (bottom) regions. The intensity scale of the downfield region is increased in order to show the resonances clearly.

(B) Concentrations of the metabolites that show statistically significant differences ($p < 0.05$) between the WT (green) and ID mutant (red) cells. For plotting convenience, the concentrations of oxypurinol shown are 10-fold lower than the actual concentrations.

(C) Schematic diagram of the metabolic pathways affected by the RECQ4 ID mutant. The red and blue arrows represent increased and decreased metabolite concentrations, respectively, in the ID mutant cells compared with the WT cells.

The Interaction of the Lymphoma-Associated RECQ4 ID Mutant Protein with MT p32 Is Defective

We next determined whether the interaction of RECQ4 with PP2A, NPM, or p32 was altered by the RECQ4 ID mutation. We found that PP2A and NPM copurified with both the RECQ4 WT and ID proteins, but p32 failed to copurify with the ID mutant (Figures 6A, S5E, and S5F). The loss of the p32 interaction coincided with a significant increase of the MT replication helicase PEO1 in the purified RECQ4 ID complexes (Figures 6A, S5E, and S5F). This result suggested the possibility that the interaction of RECQ4 with p32 and PEO1 is mutually exclusive. Using purified recombinant GST-p32 or GST-PEO1 bound to glutathione beads, incubated with either purified recombinant RECQ4 WT and ID mutant protein (Figure 6B), we confirmed that GST-p32 was able to directly interact with RECQ4 WT, but not the ID mutant (Figure 6C, lanes b and c). Furthermore, the interaction with p32 mapped to the RECQ4 N terminus (Figure 6B, 1–492 aa; Figure 6C, lane e), which contains the 44 amino acids that are missing in the ID mutant. In contrast, both RECQ4 WT and ID mutant interacted with PEO1 (Figure 6C, lanes f and g). Even though the N-terminal fragment of RECQ4 exhibited a strong interaction with PEO1, a weaker interaction was also detected using a C-terminal fragment in vitro (Figure 6B, 450–1,208 aa; Figure 6C, lanes h and i).

To test whether p32 can affect the interaction between RECQ4 and PEO1, we incubated purified recombinant PEO1 protein tagged with chitin-binding domain (CBD) and anchored on chitin beads with recombinant RECQ4, p32, or the RECQ4-p32

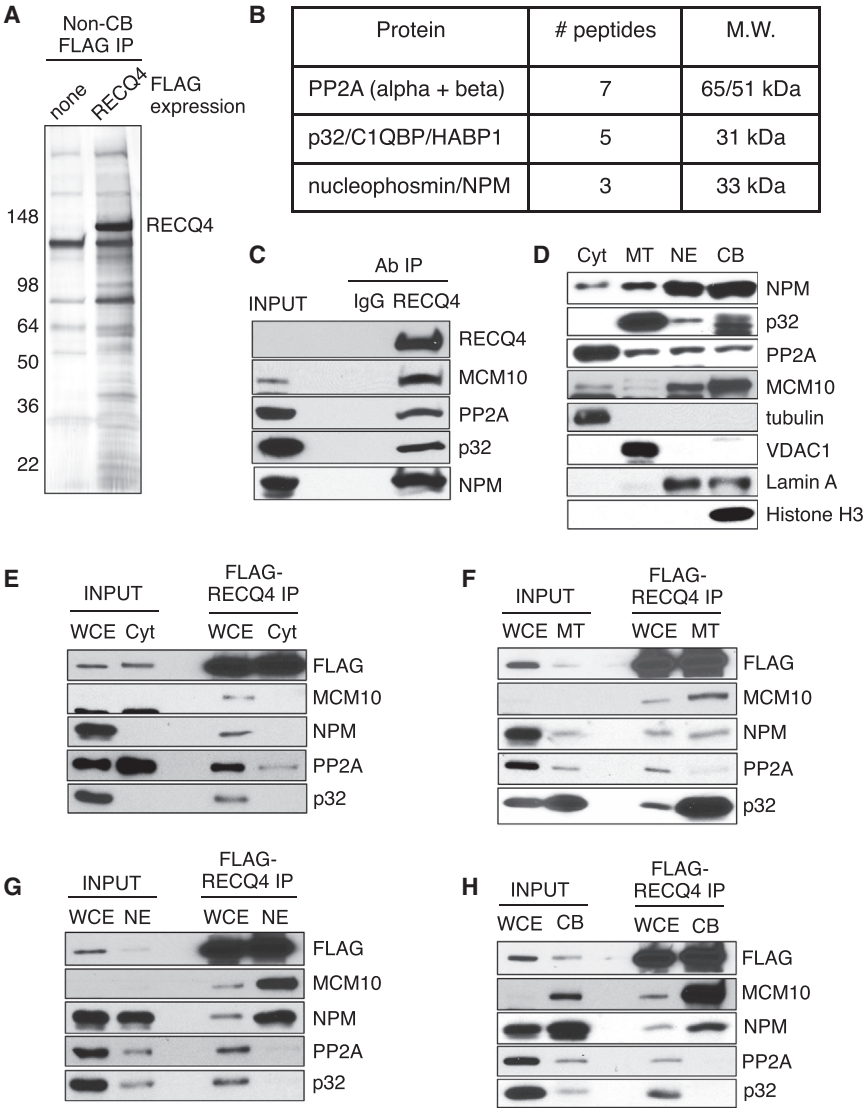

Protein	# peptides	M.W.
PP2A (alpha + beta)	7	65/51 kDa
p32/C1QBP/HABP1	5	31 kDa
nucleophosmin/NPM	3	33 kDa

Figure 5. Distinct RECQ4 Protein Complexes Identified from Different Cellular Compartments

(A) Purification and identification of non-CB FLAG-RECQ4 complexes from human cells. The immunopurified FLAG-RECQ4 complexes were separated on 4%–15% gradient SDS-PAGE and then silver stained.

(B) List of the polypeptides that were reproducibly identified in non-CB RECQ4 complexes by mass spectrometry (left), the number of peptides detected (center), and their corresponding molecular weight (right). Only those polypeptides that were not present in the control immunoprecipitation without FLAG expression and were specific to the RECQ4 complex are listed.

(C) Western blots of the input (left) and immunopurified protein complexes isolated using control IgG (center) or RECQ4-specific antibodies (right), probed with antibodies to detect RECQ4, MCM10, PP2A, NPM, and p32.

(D) The protein levels of NPM, p32, PP2A, and MCM10 were analyzed on western blots of Cyt, MT, NE, and soluble CB fractions prepared from HEK293T cells. Tubulin, VDAC1, Lamin A, and Histone H3 were used as markers for Cyt, MT, NE, and CB, respectively.

(E–H) Western blots of the input (left 2 lanes) and FLAG-RECQ4 WT complexes immunopurified (right two lanes) from WCEs and (E) Cyt, (F) MT, (G) NE, and (H) CB fractions probed with antibodies to detect the presence of RECQ4, MCM10, PP2A, NPM, and p32.

complex. As expected, CBD-PEO1 was able to pull down FLAG-RECQ4, but it failed to do so when RECQ4 was preincubated with p32 (Figure 6D, compare lanes e and g). In contrast, MCM10, which interacts with the N terminus of RECQ4 (Xu et al., 2009), did not block the RECQ4-PEO1 interaction (Figure 6D, compare lanes e and i). Interestingly, we found that PEO1 also interacted directly with p32 and MCM10 in vitro, but only the PEO1-p32 interaction was significantly weakened in the presence of RECQ4 (Figure 6D, lanes f–i). These results reveal a unique function for p32 in negatively regulating the RECQ4-PEO1 interaction.

p32 Negatively Regulates Transport of RECQ4 to MT

Next, we tested whether p32 plays a role in controlling the transport of RECQ4 to the MT. Indeed, depleting p32 by small interfering RNA (siRNA) increased the amount of RECQ4 and MCM10 in MT, and there was a corresponding decrease in nuclear RECQ4 and MCM10 levels (Figures 7A and 7B). Interestingly, in NPM-depleted cells, p32 accumulated in the Cyt fraction, which resulted in a modest decrease in the amount of MT p32 (Figure 7C). This observation reveals an unexpected functional interaction between NPM and p32 that has not been previously described, and provides an explanation for the slight but noticeable increase of RECQ4 in the MT of NPM knockdown cells (Figure 7A). Importantly, because the RECQ4 ID mutant protein failed to interact with p32, it could no longer be regulated by p32, and therefore, as expected, depleting p32 had little effect on the localization and accumulation of the RECQ4 ID mutant to the MT (Figure 7A). Indeed, in contrast to what was observed for cells expressing RECQ4 WT proteins, depleting p32 from cells expressing the RECQ4 ID mutant did not significantly increase the mtDNA copy number (Figure 7D). Altogether, these results demonstrate a function for p32 in controlling the amount of RECQ4 that is transported to the MT.

DISCUSSION

Synthesis of nuclear DNA and mtDNA is known to be coordinated during the cell cycle (Chatre and Ricchetti, 2013). Mammalian RECQ4 is an essential enzyme that is involved in the synthesis of both nuclear DNA and mtDNA (Croteau et al., 2012; Liu,

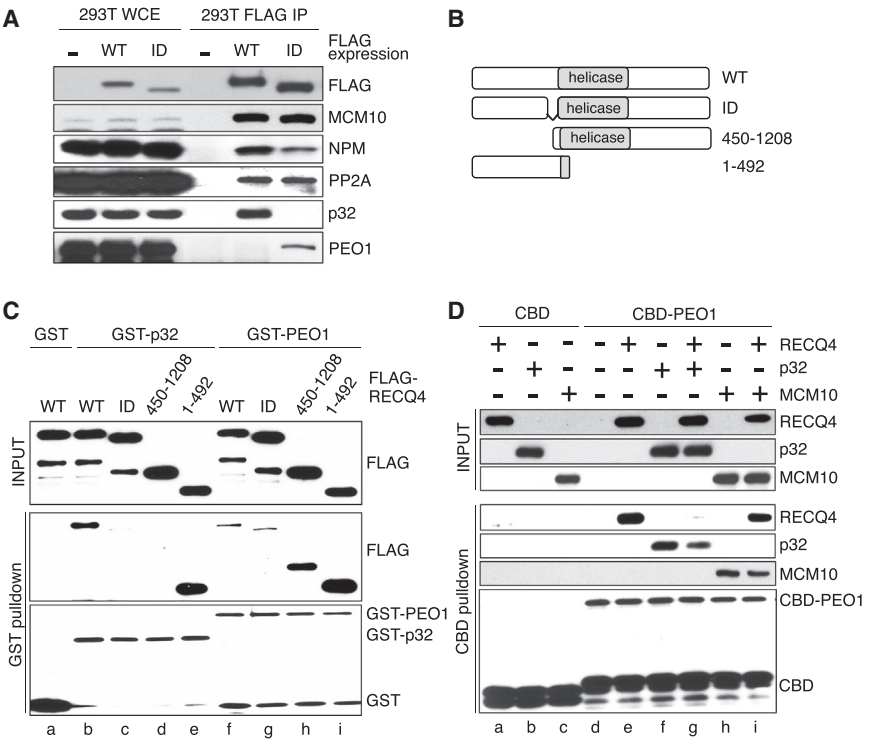

Figure 6. The Lymphoma-Associated RECQ4 ID Mutant Cannot Interact with p32

(A) Western blots of the immunopurified FLAG complexes from WCEs (left three lanes) prepared from cells expressing vector, FLAG-RECQ4 WT, or FLAG-RECQ4 ID. The immunopurified complexes were probed with antibodies to detect RECQ4, MCM10, NPM, PP2A, p32, and PEO1.

(B) Schematic diagrams of RECQ4 WT and fragments used in the in vitro pull-down experiments shown in (C). The conserved SFII helicase domain is shown in light gray.

(C) Western blots of the recombinant FLAG-RECQ4 WT and fragments before (upper) and after (center) pull-down, using purified recombinant GST, GST-p32, and GST-PEO1 (bottom) bound to the glutathione beads.

(D) Western blots of the recombinant FLAG-RECQ4, GST-p32, and GST-MCM10 before (upper three panels) and after (center three panels) pull-down using purified recombinant CBD and CBD-PEO1 bound to the chitin beads (bottom panel).

tling system between MT and the nucleus. In support of this, p32 promotes the nuclear import of adenovirus core protein V (Matthews and Russell, 1998) 2010). Our study demonstrates that the Ala420–Ala463 residues, which are missing in the most common and highly cancer-prone RECQ4 ID mutation, play a crucial role in balancing the distribution of RECQ4 between the nucleus and MT, and provides an explanation for the decreased nuclear retention observed previously for this RECQ4 mutant (Burks et al., 2007). We provide evidence that supports our conclusion that the excess RECQ4 ID mutant proteins found in the MT were transported from the nucleus. First, the increased amount of RECQ4 ID mutant protein in the MT was accompanied by decreased levels of CB ID protein (Figures 2E, 2F, 3B, and 3C). Second, MCM10, which is the primary protein that interacts with RECQ4 on human chromatin, also showed increased MT localization in RECQ4 ID cells (Figure 3C). Finally, we identified three proteins (PP2A, NPM, and p32) that interacted with RECQ4 in various cellular compartments (Figure 5), and showed that the RECQ4 ID mutant cannot bind to p32 in human cells (Figure 6A). Loss of p32 binding led to an accumulation of the RECQ4 mutant protein in the MT, an enhanced level of interaction of RECQ4 ID with the MT replication helicase PEO1, and increases in mtDNA synthesis. Consistent with a role for p32 as a negative regulator of RECQ4 transport from the nucleus to the MT, depletion of p32 is also sufficient to disrupt the balance of the CB and MT distribution of WT RECQ4 and MCM10 (Figures 7A and 7B).

Future work is needed to define the exact molecular mechanism by which p32 prevents RECQ4 and MCM10 from localizing to the MT. p32 is also known to localize to the nucleus, although to a lesser extent, and participate in cellular processes that involve nuclear proteins (Brokstad et al., 2001). Possibly, RECQ4 and MCM10 transiently interact with p32 in the nucleus. We suggest that p32 could be a component of the protein-shut- and translocation of the tumor suppressor ARF to MT to activate p53-dependent apoptosis (Itahana and Zhang, 2008). Alternatively, the interaction of RECQ4 with p32 at MT may provide a negative feedback signal or prevent interaction with other MT protein(s), such as PEO1, whose interaction with RECQ4 is mutually exclusive to p32 (Figure 6D), to limit the MT association and entry of RECQ4.

Interestingly, even though both RECQ4 and MCM10 can be found in MT, only the RECQ4 protein was transported into the MT matrix, and MCM10 remained mostly at the outer MT membrane (Figure 3C). It is possible that upon being transported to the MT, RECQ4 dissociates from MCM10 via other protein-protein interaction(s), such as with PEO1. However, when we tested the possibility that PEO1 disrupts the RECQ4-MCM10 interaction in vitro, we found this was not the case (Figure 6D). Alternatively, posttranslational modifications might play a role in modulating the localization and interactions of RECQ4 with other proteins. In support of this, we have shown that the RECQ4-MCM10 interaction may be disrupted by potential CDK-dependent phosphorylation (Xu et al., 2009). We also observed that RECQ4 was present in multiple phosphorylation states in vivo (J.-T.W. and Y.L., unpublished data). Similarly, RECQ4 phosphorylation may also regulate the p32-RECQ4 interaction to allow a limited amount of RECQ4 to enter MT and promote mtDNA synthesis.

In addition to MCM10, RECQ4 promotes the MT localization of the p53 tumor suppressor (De et al., 2012). In this study, we found that although the RECQ4 ID mutant accumulated in the MT, the p53 level in MT was unaffected (Figures 3B and 3C). It is worth mentioning that NPM blocks p53 from being transported to the MT (Dhar and St Clair, 2009). Therefore, it would be of

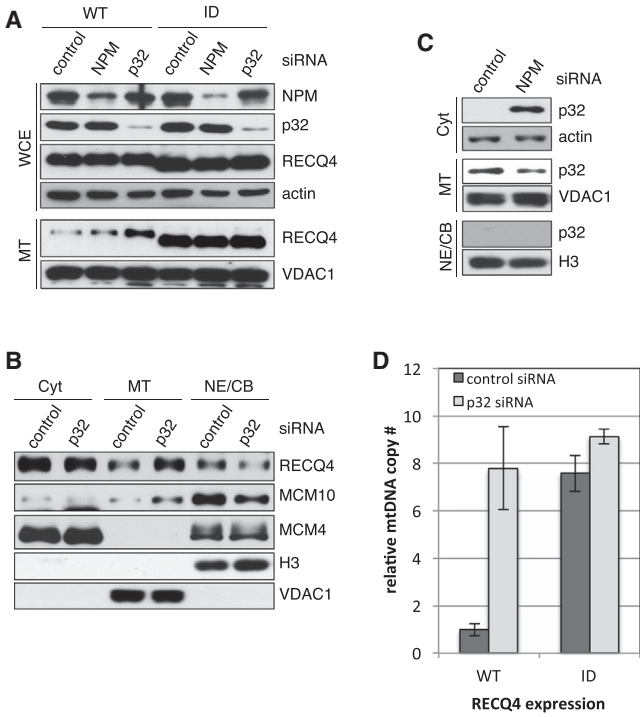

Figure 7. The Lymphoma-Associated RECQ4 ID Mutant Cannot Be Regulated by MT p32

(A) The protein levels of NPM, p32, and RECQ4 were analyzed on western blots of WCE (top four panels) and MT (bottom two panels) prepared from HEK293T cells that expressed either RECQ4 WT or ID proteins and were treated with control, NPM, or p32 siRNA. Actin and VDAC1 were used as loading controls for WCE and MT, respectively.

(B) Protein levels of RECQ4 and MCM10 in Cyt, MT, and NE/CB fractions prepared from control or p32 siRNA-treated cells were analyzed on western blots. MCM4, VDAC1, and Histone H3 were used as loading controls.

(C) Protein levels of p32 in Cyt, MT, and NE/CB fractions prepared from control or NPM siRNA-treated cells were analyzed on western blots. Actin, VDAC1, and Histone H3 were used as loading controls.

(D) The copy number of mtDNA relative to genomic DNA was quantified in RECQ4 WT and ID cells that were transfected with control or p32 siRNA. Results are represented as means ± SD from three independent experiments.

great interest to test whether NPM prevents p53 MT transport through its interaction with RECQ4. This possibility would explain why p53 levels at the MT were unaffected in RECQ4 ID cells, because the RECQ4 ID mutant remained capable of interacting with NPM (Figure 6A).

In this study, we also revealed an unexpected functional interaction between p32 and NPM. We showed that NPM prevented the loss of p32 in MT and its accumulation in the Cyt (Figure 7C). Cumulative studies provide evidence that both NPM and p32 interact with the ARF tumor suppressor (Chen et al., 2010; Itahana and Zhang, 2008), which is required for p53-mediated apoptosis. p32 promotes ARF localization to the MT, which sensitizes the cells to p53-induced apoptosis (Itahana and Zhang, 2008). In the nucleus, NPM abolishes ULF-mediated degradation of ARF to activate the p53-mediated stress response (Chen et al., 2010). Further studies are needed to determine whether NPM has a direct role in shuttling p32 from the Cyt to the MT or the shuttling is indirectly regulated through common interacting proteins, such as RECQ4 or ARF.

In summary, the importance of the interaction between p32 and RECQ4 is illustrated by the fact that the highly cancer-prone RECQ4 ID mutant failed to interact with p32, leading to increases in mtDNA copy number and MT dysfunction. Alterations to mtDNA content in cells can have profound effects on aging and human diseases, including cancers. This study provides insight into the links between RECQ4 mutations and both aging and cancer etiology.

EXPERIMENTAL PROCEDURES

Plasmids and Proteins

The shRNA expression plasmid pInduceMir3 was kindly provided by Dr. Stephen J. Elledge (Harvard University). To generate the pInduceMir3-RECQ4-shRNA plasmid, a DNA fragment containing the sequence 5′-TGCTGTTGACAGTGAGCGCCGGCTCAACATGAAGCAGAAATAGTGAAGCCACAGATGTATTTCTGCTTCATGTTGAGCCGTTGCCTACTGCCTCGGA-3′ was PCR amplified and cloned into pInduceMir3 between the XhoI and EcoRI sites. The pCMV-FLAG-RECQ4 was generated as previously described (Xu et al., 2009). The shRNA-resistant FLAG-RECQ4 expressing plasmid pCMV-FLAG-RECQ4-R was generated by mutagenesis using the oligo 5′-ACAGGGGCAATTACGTTAGATTGAATATGAAACAAAAGCACTACGTGCGGGGCC-3′, and pCMV-FLAG-RECQ4 as the template. The mutagenesis primer 5′-CCAGTGTCCCCGGCCAGAGACGCCGGCTGAGG-3′ was used to generate shRNA-resistant pCMV-FLAG-RECQ4ID-R using pCMV-FLAG-RECQ4-R as the template, and pET16b-RECQ4ID-FLAG using pET16b-RECQ4-FLAG as the template (Xu and Liu, 2009). pET16b-RECQ(450-1208)-FLAG and pET16b-RECQ4(1-492)-FLAG were generated as previously described (Xu and Liu, 2009). The mutagenesis primer 5′-GCCTACAGGTGCCGGCAGGTCCCTGTGCTACCAGC-3′ was used to generate pET16b-RECQ4ID(K508R)-FLAG. To generate pGEX4T1-p32 or pGEX4T1-PEO1, p32 or PEO1 was PCR amplified from the 293T cDNA library and cloned into pGEX4T-1 (GE Healthcare) between the EcoRI and XhoI sites. pGEX4T1-MCM10 was generated as described previously (Xu et al., 2009). To generate pTXB1-PEO1, PEO1 was cloned into pTXB1 (New England BioLabs) between NdeI and XhoI sites. N-terminal His-tagged and C-terminal FLAG-tagged WT RECQ4, RECQ4ID, RECQID(K508R), RECQ(450-1208), and RECQ4(1-492) proteins were purified as previously described (Xu and Liu, 2009). GST-p32, GST-PEO1, and GST were purified as previously described for GST-MCM10 purification (Xu and Liu, 2009). CBD-PEO1 and CBD were expressed in Rosetta (DE3) pLysS cells by inducing with 0.1 mM isopropyl-β-D-thio-galactoside overnight at 4°C. Cell pellets were resuspended in buffer C (20 mM Tris pH8.0, 500 mM NaCl, 1 mM EDTA, 0.1% Triton X-100) plus 0.2 mg/ml lysozyme and 1× protease inhibitor cocktail (Roche), and lysed by sonication. After centrifugation, the supernatant was incubated with Chitin beads (New England BioLabs) for 2 hr at 4°C. The beads were washed extensively with buffer C and stored in buffer B (50 mM Tris pH 8.0, 300 mM NaCl, 50% glycerol, 1 mM dithiothreitol [DTT], 1% Triton X-100).

Antibodies

Rabbit anti-FLAG (F7425) was purchased from Sigma. Goat anti-Actin (sc1616), mouse anti-p53 (DO-1) (sc-126), rabbit anti-NPM (sc-5564), rabbit anti-Histone H3 (sc-10809), rabbit anti-CDC45 (sc-20685), mouse anti-CDC6 (sc-9964), mouse anti-α tubulin (sc-8035), mouse anti-GST (sc-138), and rabbit anti-Lamin A/C (sc-20681) were purchased from Santa Cruz. Rabbit anti-VDAC1 (ab15895) and rabbit anti-MCM7 (ab52489) were purchased from Abcam. Rabbit anti-p32 (6502S) and rabbit anti-PP2Aα subunit (2039S) were purchased from Cell Signaling Technology. Rabbit anti-RECQ4 (2547.00.02) that was used in the coimmunoprecipitation experiments (Figure 5C) and rabbit anti-SLD5 were purchased from Strategic Diagnositics. Rat anti-BrdU (MCA2060T) was purchased from AbD Serotec. Rabbit anti-MCM10 (12251-1-AP) and rabbit anti-PSF2 (16247-1-AP) were purchased from Proteintech Group. Rabbit anti-MCM4 (A300-193A) was

purchased from Bethyl Laboratories. Rabbit anti-PEO1 (ARP36483_P050) was purchased from AVIVA Systems Biology. Mouse anti-p84 (GTX70220) was purchased from GeneTex. Mouse anti-CBD (E80345) was purchased from New England Biolabs. Rabbit anti-dimethyl-Histone H3 (Lys36) (07-274) was purchased from Millipore. Rabbit anti-RECQ4 used in western blot analyses (Figures 2A, 2C, 5C, S1, S2A, and S2C) was generated as previously described (Xu et al., 2009). Rabbit anti-MT single-stranded binding protein (anti-mtSSB) was kindly provided by Dr. Valeria Tiranti (IRCCS Foundation Neurological Institute, Milan, Italy).

Cell Culture, siRNA, and Cell Proliferation Assay

All cells were cultured in Dulbecco's modified Eagle's medium supplemented with 10% fetal bovine serum and streptomycin/penicillin (100 U/ml). NPM stealth siRNA 5′-UGCAAAGGAUGAGUUGCACAUUGUU-3′ and p32 stealth siRNA 5′-GACGAGGCUGAGAGUGACAUCUUCU-3′ were purchased from Invitrogen. The siRNAs (25 nM) were transfected using DharmaFECT 1 transfection reagent (Thermo Fisher Scientific) for 48 hr according to the manufacturer's protocol. Stable shRNA-expressing cell lines were established by transfecting the pInduceMir3 vector or pInduceMir3-RECQ4-shRNA, and selecting with 2 μg/ml puromycin. To establish WT FLAG-RECQ4 and ID stable 293T cell lines, the RECQ4 shRNA stable cell line was cotransfected with pIREShyg3 (Clontech) and either pCMV-FLAG-RECQ4-R or pCMV-FLAG-RECQ4ID-R plasmid, and then selected with 200 μg/ml hygromycin. To establish WT FLAG-RECQ4 and ID stable U2OS and HT1080 cell lines, the RECQ4 shRNA stable cell line was transfected with pCMV-FLAG-RECQ4-R or pCMV-FLAG-RECQ4ID-R plasmid, and then transformed cells were selected using 400 μg/ml G418. Single clones were picked and screened on western blots probed with the appropriate antibodies. Positive clones were further amplified to establish stable cell lines. Crystal violet cell proliferation assays were performed as previously described (Kueng et al., 1989).

ATPase and DNA Strand-Exchange Assays

DNA unwinding assays were performed as previously described (Xu and Liu, 2009). The ATPase activity was measured by incubating the purified recombinant RECQ4 proteins with 8 pmol ssDNA and 2.5 × 10^2 μCi [γ-^{32}P] ATP in a 10 μl reaction containing ATPase buffer (30 mM Tris pH 7.5, 10% glycerol, 5 mM $MgCl_2$, 50 μM cold ATP, 1 mM DTT, 100 μg/ml BSA) for 1 hr at 37°C. The reactions were stopped by adding 5 μl of 0.5 M EDTA and separated by PEI-cellulose thin-layer chromatography plate using a solution of 0.8 M LiCl and 1 M formic acid, and incubation in a moist chamber for 1.5 hr. The percentage of ATPase hydrolysis was quantified using a phosphoimager.

Cell Fractionation, Immunopurification, and Mass Spectrometry Analysis

Cells were fractionated into Cyt, NE, and benzonase-treated soluble CB fractions as previously described (Xu et al., 2009). To isolate the MT fraction, the cell pellet was resuspended in MT buffer (210 mM sucrose, 70 mM mannitol, 1 mM EDTA, 1 mM EGTA, 1.5 mM $MgCl_2$, 10 mM HEPES [KOH] pH 7.2) that contained EDTA-free protease inhibitors and phosphatase inhibitors, and incubated on ice for 30 min. After homogenization, cell lysates were centrifuged at 1,000 *g* for 5 min to pellet the intact cells and nuclei. The supernatant was further centrifuged at 10,000 *g* to pellet the MT-enriched heavy membrane fraction. The supernatant was collected as Cyt without MT. The MT-enriched pellet was washed with MT buffer twice, resuspended in MT lysis buffer (20 mM HEPES pH 7.9, 1.5 mM $MgCl_2$, 1 mM EDTA, 150 mM KCl, 0.1% NP40, 1 mM DTT, 10% glycerol) that contained 0.15 U/μl benzonase and EDTA-free protease inhibitors and phosphatase inhibitors, sonicated, and incubated on ice for 1 hr. The supernatant was collected as the MT fraction. For trypsin analysis, intact MT were isolated and incubated with 100 μg/ml trypsin in MT buffer for 20 min on ice. The trypsin-treated MT were recovered by centrifuging, and trypsin was inactivated by adding 1× SDS-PAGE loading buffer. Immunopurification and mass spectrometry analysis of the FLAG-tagged RECQ4 and the endogenous RECQ4 complexes were performed as previously described (Xu et al., 2009).

mtDNA Copy Number

Total cellular DNA was isolated using the DNeasy Blood & Tissue Kit (QIAGEN). Genomic DNA (Lamin B origin) and mtDNA (D-Loop) were quantified by real-time PCR using the SYBR Green (Power) PCR Master Mix (Life Technologies) and the ABI 7500 Fast Real-Time PCR System. All reactions were run in triplicate. Relative mtDNA copy numbers were normalized with genomic DNA (Lamin B origin). The D-loop PCR primers were 5′-GTGGCTTTGGAGTTG CAGTT-3′ and 5′-GAAGCAGATTTGGGTACCAC-3′. The Lamin B origin primers were 5′-ATGAAGCGGATGTCTAAGAAAG-3′ and 5′-CGCCTGGGTCC TGTTTACAC-3′.

mtDNA Synthesis

RECQ4 shRNA-resistant expressing plasmids pCMV-FLAG-RECQ4-R and pCMV-FLAG-RECQ4ID-R were transfected into RECQ4 shRNA cells with continuum transfection reagent (Gemini Bio). After 48 hr, cells were further incubated with or without 30 μM BrdU for 4 hr. To prepare mtDNA, cells were harvested and MT were isolated as described above. The MT were then resuspended in DNA isolation buffer (10 mM Tris pH 8.0, 10 mM EDTA, 0.5% SDS buffer, and 100 μg/ml protease K), incubated at 45°C for 5 hr, phenol-chloroform extracted, and ethanol precipitated. The presence of genomic DNA contaminants was excluded by performing PCR analysis of Lamin B gene using the primers 5′-CTGCAGCTGGGGCTGGCATG-3′ and 5′-GACATCCGCTTCATTAGGGCAG-3′ for the LAMIN B Ori locus (Xu et al., 2009). The indicated amounts of mtDNA were blotted onto a nitrocellulose membrane and vacuum dried for 2 hr at 80°C as previously described (Brown, 2001). The membrane was then probed with mouse BrdU antibody (MD5100; Invitrogen) and washed as for western blotting.

Metabolite Measurement

The metabolites from the cells transfected with RECQ4 WT and ID mutant were extracted as previously described (Cano et al., 2010). The lyophilized, water-soluble metabolites were resuspended in 100% D_2O containing 3.2 μM 4,4-dimethyl-4-silapentane-1-sulfonic acid (DSS), which served as the ^{1}H chemical-shift reference and an internal concentration standard. Three replicates were prepared. NMR spectra were acquired at 25°C on a Bruker Avance III spectrometer equipped with a cryoprobe operating at a 700.243 MHz ^{1}H frequency. ^{1}H NMR spectra were acquired with water presaturation during relaxation delay and using a spoil gradient over 32 k data points, spectral width of 13 kHz, 3 s relaxation delay, and 2,048 scans. The NMR spectra were processed using the Chenomx NMR Suite Processor (version 7.1; Chenomx). The Chenomx NMR Suite Profiler software was used to identify and quantify the metabolites. The concentrations of the metabolites were converted from micromolar units to nanomoles by multiplying the sample volume and adjusting for the number of cells in the sample.

Protein Interactions In Vitro

GST, GST-p32, GST-PEO1, or GST-MCM10 (4 nmol) bound to glutathione beads was blocked with 1 mg/ml BSA in buffer D (40 mM Tris pH 7.4, 10% glycerol, 0.1% Triton X-100, 1 mM EDTA, 150 mM NaCl, 1 mM DTT) for 1 hr at 4°C. His- and FLAG-tagged RECQ4 full-length (FL) and fragments (0.4 nmol) were added and incubated for 2 hr at 4°C. The bound proteins were washed extensively with buffer D, boiled in SDS sample buffer, separated by SDS-PAGE, and analyzed on western blots. For in vitro competition assays, the His- and FLAG-tagged RECQ4 FL (0.5 nmol) were incubated with or without p32 or MCM10 (0.5 nmol) in the presence of 2 μg BSA for 1.5 hr at 4°C. They were then added to the BSA-blocked CBD of CBD-PEO1 (0.5 nmol) bound chitin beads and incubated for another 1.5 hr at 4°C. The bound proteins were washed extensively with buffer D, boiled in SDS sample buffer, separated on SDS-PAGE, and analyzed on western blots.

SUPPLEMENTAL INFORMATION

Supplemental Information includes Supplemental Experimental Procedures and seven figures and can be found with this article online at http://dx.doi.org/10.1016/j.celrep.2014.03.037.

ACKNOWLEDGMENTS

We thank Dr. Margaret Morgan for her comments and expert editing of this manuscript. This work was supported by NIH grant R01 CA151245, a Yale Comprehensive Cancer Center pilot research grant, and an Elsa U. Pardee Foundation research grant to Y.L. The NMR study was supported by NIH grant R01 GM 086171 to Y.C.

Received: June 28, 2013
Revised: January 6, 2014
Accepted: March 12, 2014
Published: April 17, 2014

REFERENCES

Abe, T., Yoshimura, A., Hosono, Y., Tada, S., Seki, M., and Enomoto, T. (2011). The N-terminal region of RECQL4 lacking the helicase domain is both essential and sufficient for the viability of vertebrate cells. Role of the N-terminal region of RECQL4 in cells. Biochim. Biophys. Acta *1813*, 473–479.

Brokstad, K.A., Kalland, K.H., Russell, W.C., and Matthews, D.A. (2001). Mitochondrial protein p32 can accumulate in the nucleus. Biochem. Biophys. Res. Commun. *281*, 1161–1169.

Brown, T. (2001). Dot and slot blotting of DNA. Curr. Protoc. Mol. Biol. *Chapter 2*, Unit 2.9B.

Burks, L.M., Yin, J., and Plon, S.E. (2007). Nuclear import and retention domains in the amino terminus of RECQL4. Gene *391*, 26–38.

Cano, K.E., Li, Y.J., and Chen, Y. (2010). NMR metabolomic profiling reveals new roles of SUMOylation in DNA damage response. J. Proteome Res. *9*, 5382–5388.

Carew, J.S., Nawrocki, S.T., Xu, R.H., Dunner, K., McConkey, D.J., Wierda, W.G., Keating, M.J., and Huang, P. (2004). Increased mitochondrial biogenesis in primary leukemia cells: the role of endogenous nitric oxide and impact on sensitivity to fludarabine. Leukemia *18*, 1934–1940.

Chatre, L., and Ricchetti, M. (2013). Prevalent coordination of mitochondrial DNA transcription and initiation of replication with the cell cycle. Nucleic Acids Res. *41*, 3068–3078.

Chen, D., Shan, J., Zhu, W.G., Qin, J., and Gu, W. (2010). Transcription-independent ARF regulation in oncogenic stress-mediated p53 responses. Nature *464*, 624–627.

Chi, Z., Nie, L., Peng, Z., Yang, Q., Yang, K., Tao, J., Mi, Y., Fang, X., Balajee, A.S., and Zhao, Y. (2012). RecQL4 cytoplasmic localization: implications in mitochondrial DNA oxidative damage repair. Int. J. Biochem. Cell Biol. *44*, 1942–1951.

Croteau, D.L., Rossi, M.L., Canugovi, C., Tian, J., Sykora, P., Ramamoorthy, M., Wang, Z.M., Singh, D.K., Akbari, M., Kasiviswanathan, R., et al. (2012). RECQL4 localizes to mitochondria and preserves mitochondrial DNA integrity. Aging Cell *11*, 456–466.

D'Souza, A.D., Parikh, N., Kaech, S.M., and Shadel, G.S. (2007). Convergence of multiple signaling pathways is required to coordinately up-regulate mtDNA and mitochondrial biogenesis during T cell activation. Mitochondrion *7*, 374–385.

De, S., Kumari, J., Mudgal, R., Modi, P., Gupta, S., Futami, K., Goto, H., Lindor, N.M., Furuichi, Y., Mohanty, D., and Sengupta, S. (2012). RECQL4 is essential for the transport of p53 to mitochondria in normal human cells in the absence of exogenous stress. J. Cell Sci. *125*, 2509–2522.

de Souza-Pinto, N.C., Aamann, M.D., Kulikowicz, T., Stevnsner, T.V., and Bohr, V.A. (2010). Mitochondrial helicases and mitochondrial genome maintenance. Mech. Ageing Dev. *131*, 503–510.

Dhar, S.K., and St Clair, D.K. (2009). Nucleophosmin blocks mitochondrial localization of p53 and apoptosis. J. Biol. Chem. *284*, 16409–16418.

Falini, B., Nicoletti, I., Bolli, N., Martelli, M.P., Liso, A., Gorello, P., Mandelli, F., Mecucci, C., and Martelli, M.F. (2007). Translocations and mutations involving the nucleophosmin (NPM1) gene in lymphomas and leukemias. Haematologica *92*, 519–532.

Fogal, V., Richardson, A.D., Karmali, P.P., Scheffler, I.E., Smith, J.W., and Ruoslahti, E. (2010). Mitochondrial p32 protein is a critical regulator of tumor metabolism via maintenance of oxidative phosphorylation. Mol. Cell. Biol. *30*, 1303–1318.

Ichikawa, K., Noda, T., and Furuichi, Y. (2002). [Preparation of the gene targeted knockout mice for human premature aging diseases, Werner syndrome, and Rothmund-Thomson syndrome caused by the mutation of DNA helicases]. Nippon Yakurigaku Zasshi *119*, 219–226.

Im, J.S., Ki, S.H., Farina, A., Jung, D.S., Hurwitz, J., and Lee, J.K. (2009). Assembly of the Cdc45-Mcm2-7-GINS complex in human cells requires the Ctf4/And-1, RecQL4, and Mcm10 proteins. Proc. Natl. Acad. Sci. USA *106*, 15628–15632.

Itahana, K., and Zhang, Y. (2008). Mitochondrial p32 is a critical mediator of ARF-induced apoptosis. Cancer Cell *13*, 542–553.

Janssens, V., and Goris, J. (2001). Protein phosphatase 2A: a highly regulated family of serine/threonine phosphatases implicated in cell growth and signalling. Biochem. J. *353*, 417–439.

Jeng, J.Y., Yeh, T.S., Lee, J.W., Lin, S.H., Fong, T.H., and Hsieh, R.H. (2008). Maintenance of mitochondrial DNA copy number and expression are essential for preservation of mitochondrial function and cell growth. J. Cell. Biochem. *103*, 347–357.

Jeon, J.P., Shim, S.M., Nam, H.Y., Baik, S.Y., Kim, J.W., and Han, B.G. (2007). Copy number increase of 1p36.33 and mitochondrial genome amplification in Epstein-Barr virus-transformed lymphoblastoid cell lines. Cancer Genet. Cytogenet. *173*, 122–130.

Kueng, W., Silber, E., and Eppenberger, U. (1989). Quantification of cells cultured on 96-well plates. Anal. Biochem. *182*, 16–19.

Lan, Q., Lim, U., Liu, C.S., Weinstein, S.J., Chanock, S., Bonner, M.R., Virtamo, J., Albanes, D., and Rothman, N. (2008). A prospective study of mitochondrial DNA copy number and risk of non-Hodgkin lymphoma. Blood *112*, 4247–4249.

Lee, H.C., and Wei, Y.H. (2012). Mitochondria and aging. Adv. Exp. Med. Biol. *942*, 311–327.

Lindström, M.S. (2011). NPM1/B23: A multifunctional chaperone in ribosome biogenesis and chromatin remodeling. Biochem. Res. Int. *2011*, 195209.

Liu, Y. (2010). Rothmund-Thomson syndrome helicase, RECQ4: on the crossroad between DNA replication and repair. DNA Repair (Amst.) *9*, 325–330.

Matthews, D.A., and Russell, W.C. (1998). Adenovirus core protein V interacts with p32—a protein which is associated with both the mitochondria and the nucleus. J. Gen. Virol. *79*, 1677–1685.

Muta, T., Kang, D., Kitajima, S., Fujiwara, T., and Hamasaki, N. (1997). p32 protein, a splicing factor 2-associated protein, is localized in mitochondrial matrix and is functionally important in maintaining oxidative phosphorylation. J. Biol. Chem. *272*, 24363–24370.

Sangrithi, M.N., Bernal, J.A., Madine, M., Philpott, A., Lee, J., Dunphy, W.G., and Venkitaraman, A.R. (2005). Initiation of DNA replication requires the RECQL4 protein mutated in Rothmund-Thomson syndrome. Cell *121*, 887–898.

Siitonen, H.A., Sotkasiira, J., Biervliet, M., Benmansour, A., Capri, Y., Cormier-Daire, V., Crandall, B., Hannula-Jouppi, K., Hennekam, R., Herzog, D., et al. (2009). The mutation spectrum in RECQL4 diseases. Eur. J. Hum. Genet. *17*, 151–158.

Thangavel, S., Mendoza-Maldonado, R., Tissino, E., Sidorova, J.M., Yin, J., Wang, W., Monnat, R.J., Jr., Falaschi, A., and Vindigni, A. (2010). Human RECQ1 and RECQ4 helicases play distinct roles in DNA replication initiation. Mol. Cell. Biol. *30*, 1382–1396.

Vander Heiden, M.G., Cantley, L.C., and Thompson, C.B. (2009). Understanding the Warburg effect: the metabolic requirements of cell proliferation. Science *324*, 1029–1033.

West, A.P., Shadel, G.S., and Ghosh, S. (2011). Mitochondria in innate immune responses. Nat. Rev. Immunol. *11*, 389–402.

Xu, X., and Liu, Y. (2009). Dual DNA unwinding activities of the Rothmund-Thomson syndrome protein, RECQ4. EMBO J. *28*, 568–577.

Xu, X., Rochette, P.J., Feyissa, E.A., Su, T.V., and Liu, Y. (2009). MCM10 mediates RECQ4 association with MCM2-7 helicase complex during DNA replication. EMBO J. *28*, 3005–3014.

Yin, J., Kwon, Y.T., Varshavsky, A., and Wang, W. (2004). RECQL4, mutated in the Rothmund-Thomson and RAPADILINO syndromes, interacts with ubiquitin ligases UBR1 and UBR2 of the N-end rule pathway. Hum. Mol. Genet. *13*, 2421–2430.

Ylikallio, E., Tyynismaa, H., Tsutsui, H., Ide, T., and Suomalainen, A. (2010). High mitochondrial DNA copy number has detrimental effects in mice. Hum. Mol. Genet. *19*, 2695–2705.

Yu, M. (2011). Generation, function and diagnostic value of mitochondrial DNA copy number alterations in human cancers. Life Sci. *89*, 65–71.